Supporting Information for

Elucidation of a lingual detection mechanism for high-viscosity solutions in humans

Brittany L. Miles[1], Zhenxing Wu[2], Kelly S. Kennedy[3], Kai Zhao[2], and Christopher T. Simons[1*]

[1] Department of Food Science & Technology, The Ohio State University, 2015 Fyffe Rd., Columbus, OH 43210-1007

[2] Department of Otolaryngology – Head & Neck Surgery, The Ohio State University, 915 Olentangy River Rd., Columbus, OH 43212-3153

[3] Division of Oral & Maxillofacial Surgery and Dental Anesthesiology, The Ohio State University, 305 W. 12th Avenue, Columbus, OH 43210-1267

*To whom correspondence should be addressed:

Christopher T. Simons Ph.D.
The Department of Food Science & Technology
The Ohio State University
2015 Fyffe Rd., Columbus, OH 43210-1007
Tel: 614-688-1489
Fax: 614-292-0218
Email: simons.103@osu.edu

Extended Methods

Mouthpiece Creation: The Palate-Blocked (PB) mouthpiece was created by preparing 30mL of InstaMorph moldable plastic beads (Happy Wire Dog, LLC, Scottsdale, AZ) in accordance with manufacturer's recommendations. The participant was instructed to bite down into the prepared plastic and spread it across the palate using their thumbs, making sure to cover the palate completely, until at least the first set of molars., The mouthpiece was then visually inspected by the researcher to ensure suitable coverage from the piece, and then placed into ambient temperature water until hardened. Once hardened, the participant would test fit the mouthpiece again for comfort, and if needed, was remolded using the same procedure as above.

Optical Profiling. Optical profiling via laser scanning confocal microscopy is a technique frequently used in material science to analyze surface topography during which a split laser is scanned over the surface of an object, and the amount of light refracted back to a detector is used to analyze the distance of a location on the surface from the source (1, 2). In-focus pixels

are then catalogued before the stage moves upward and the process is repeated until the entire surface has been imaged. The pixels are then used to generate a 3D model of the sample surface (see Figure S2A-C). The microscope possesses nanometer level resolution and produces color images of only slightly lesser quality to those seen in SEM (3). Unlike SEM, however, optical profilometry requires minimal prep and limits sample degradation. This process allowed for faster visualization without tissue loss. Once characterized, anatomical variation could be related to psychophysical ability, providing a concrete way to investigate the role of the filiform papillae in viscosity perception.

Biopsied samples were removed from the fixative, rinsed with DI water, and placed on a disposable, glass microscope slide for the evaluation. The slide was placed on the stage of the analyzer with the papillae oriented toward the top of the stage when possible. Eight images were taken using the associated imaging software from across the sample using 10x optical zoom being careful to minimize overlap between the images. While the majority of the samples contained only filiform papillae, a small subset of the samples (n=5) did have at least one fungiform papilla present. To ensure accurate density measurements, all images taken excluded the fungiform structures.

Papillary data were analyzed using Keyence Multifile Analyzer software (KEYENCE, Itasca, IL). Prior to measuring, all samples were corrected for surface tilt and/or general curvature. Papillary length was determined using the profile tool to draw segments from the base to tip of papillae, parallel to the direction of the papillary body using either the 2pt line tool or circle tool (Figure S1A-E). Curves were smoothed by average weight $\pm$ 2 to minimize noise in the curve coming from the roughness of the papillary surface. Finally, the Continuous Segment (CS) length tool was used to measure the length of the segment, measuring from the local minimum at the base of the papilla to the inflection point at the tip (Figure S1B). As papillae are not flat structures, taking the segment length (as opposed to the absolute distance along the X and Y planes), factored in distance in the Z plane. Papillary diameter was measured similarly, drawing a 2pt segment perpendicular to the base of the papillae inside the interpapillary furrow for base diameter and similarly perpendicular to the tip for tip diameter (Figure S1C and D). As diameter

did not depend on the surface profile, this attribute was quantified using the 2pt segment tool, measuring at the inflection point on either side of the papilla (Figure S1D). Papillary diameter was measured at both the base and the tip of the papillary structures. Three length, base diameter, and tip diameter measurements were taken per image.

Papillary density was calculated by visually identifying the number of papillae present in an image (Figure 1E). Papillae were considered separate if there was a clearly identifiable base wherein hair structures attached or if structures were clearly separated by an interpapillary furrow. Using the plane tool, count data was collected, marking each papilla with an X to prevent double counting. In the event there was an incomplete papilla, the structure was only counted if the base was in the frame. In the event only the hair structures were present, the papilla was not counted. Density was determined by dividing the count data by the area as calculated by the XY-measure function.

Solution of the Max Deflection of the Papillae. The elastic curve equation (eq (8) in the manuscript) is shown below.

$$\frac{d^2\delta}{dz^2} = \frac{M(z)}{EI(z)}$$

where M the bending moment in the papilla, I is the moment of inertia of the cross section and *E* is Young's modulus.

By considering the cone-shape model, which is shown below, and applying simple geometrical calculation, we could obtain the radius "*r*" as a function of height as

$$r(z) = r_1 + \frac{z \cdot (r_2 - r_1)}{l}$$

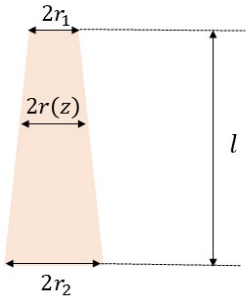

One cone-shape papilla

where r_1 and r_2 are the measured radiuses at the top and bottom of papillae, respectively.

Thus, corresponding values of area (A) and moment of inertia (I) at this cross section would be $A = \pi \cdot r^2, I = \frac{\pi \cdot r^4}{4}$. Then, the shear force *F* and moment $\bar{M}$ can be obtained according to eq (9) & eq (10) in the manuscript.

The max deflection "δ_{max}" can be solved computationally by double integrating the elastic curve equation at $z = l$. i.e.

$$\delta = \iint \frac{d^2\delta}{dz^2} dz = \iint \frac{\bar{M}(z)}{EI(z)} dz$$

$$\delta_{max} = \delta(z = l)$$

We used MATLAB to obtain the solution. The code we used is as below

```
syms z F L a pi R1 R2
%%%%%%% first integral%%%%%%%%%%%%%%%%
INT_1= int(F*(z-a)/(pi*(R1+z*(R2-R1)/L)^4/4));
c1=-subs(INT_1,z,0);
theta1=INT_1+c1;
c2=subs(theta1,z,a);
theta2=c2;

%%%%%%% second integral%%%%%%%%%%%%%%%%
INT_2= int(theta1);
c3=-subs(INT_2,z,0);
deflection1=INT_2+c3;
c4=subs (deflection1-z*c2,z,a);
deflection2=z*c2+c4;


deflection1=simplify(deflection1)
deflection2=simplify(deflection2)

% deflection1=simplifyFraction(deflection1)
% deflection2=simplifyFraction(deflection2)

deflection_max= subs(deflection2,z,L)
%%%deflection_max = -(2*F*L*a^2*(3*L^2*R1 - 3*L*R1*a +
2*L*R2*a))/(3*R1^3*pi*(R2*a - R1*a + L*R1)^2)

deflection_max_for_code= subs(deflection_max,a,z)
%%%%deflection_max_for_code = -(2*F*L*z^2*(3*L^2*R1 - 3*L*R1*z +
2*L*R2*z))/(3*R1^3*pi*(R2*z - R1*z + L*R1)^2)
%%%% need to divide Young's modulus "2600"
```

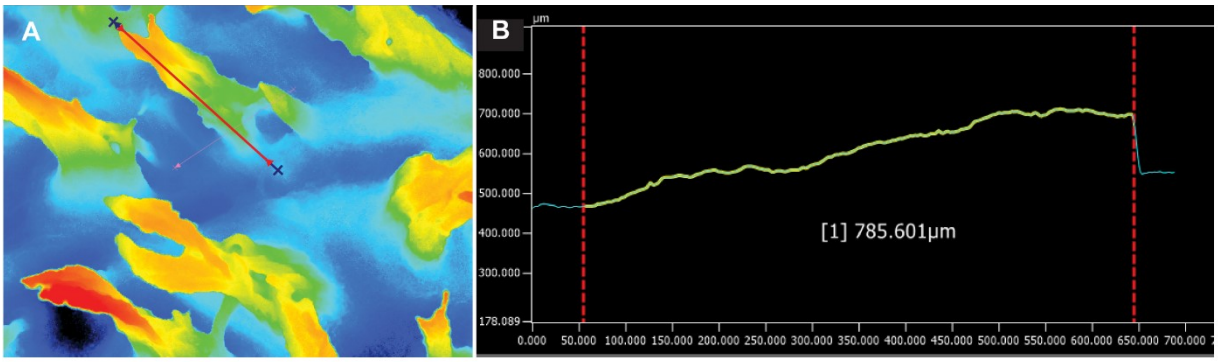

Avg. Papillary Length (Continuious Segment)

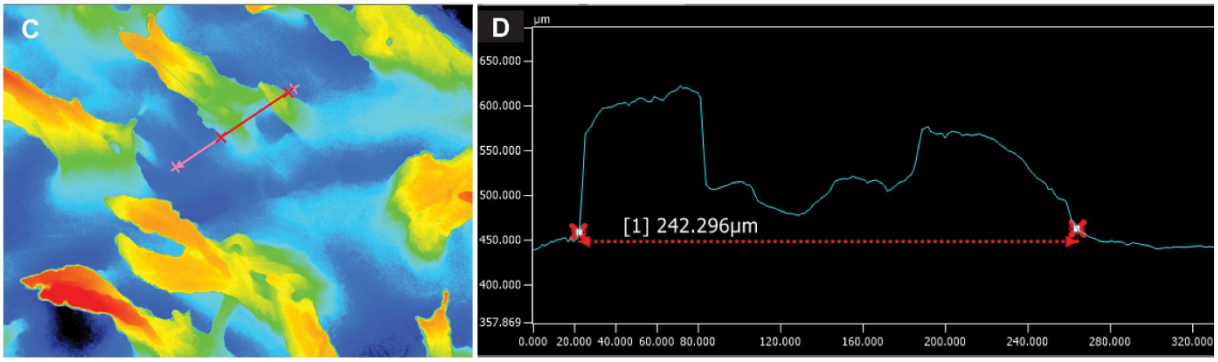

Avg. Papillary Width (2pt)

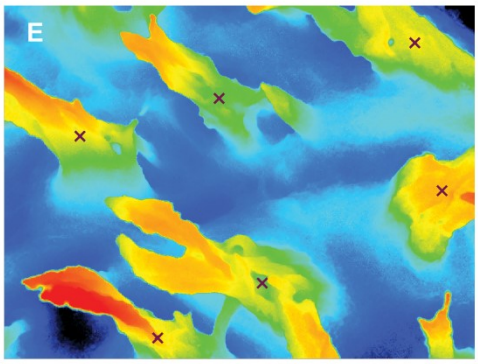

Avg. Papillary Density (Count per Area)

Figure 1A-E. Technique for biopsy analysis via optical profiling. Samples were obtained via a 5mm punch biopsy of the medial, dorsal tongue epithelium adjacent to the midline, and analyzed using optical profiling to obtain three-dimensional surface models of the tongue. Eight images were taken per sample at 10x zoom (example images: a, c, and e) and analyzed using profiling tools in Keyence Multifile Analyzer (b and d). Average papillary length was determined using the continuous segment tool (a and b), measuring for the local minimum at the base of the papillae to the inflection point, where a sudden drop in height was noted (b). Dark blue and red segments (a) correspond to the light blue profile and measured yellow segment, respectively (b). Average papillary diameter was determined using the two-point distance tool (c and d) to calculate the separation between the

inflection points on either side of the papillae (d). Pink and red segments (c) correspond to the light blue profile and measured distance between the two red X's, respectively (d). Average papillary density was measured using the count tool to count the papillae in each image (e). Partial papillae were included only if the papillary base was visible in the image. Area was standardized across counts and the mathematical average was taken across images to determine an individual's average density.

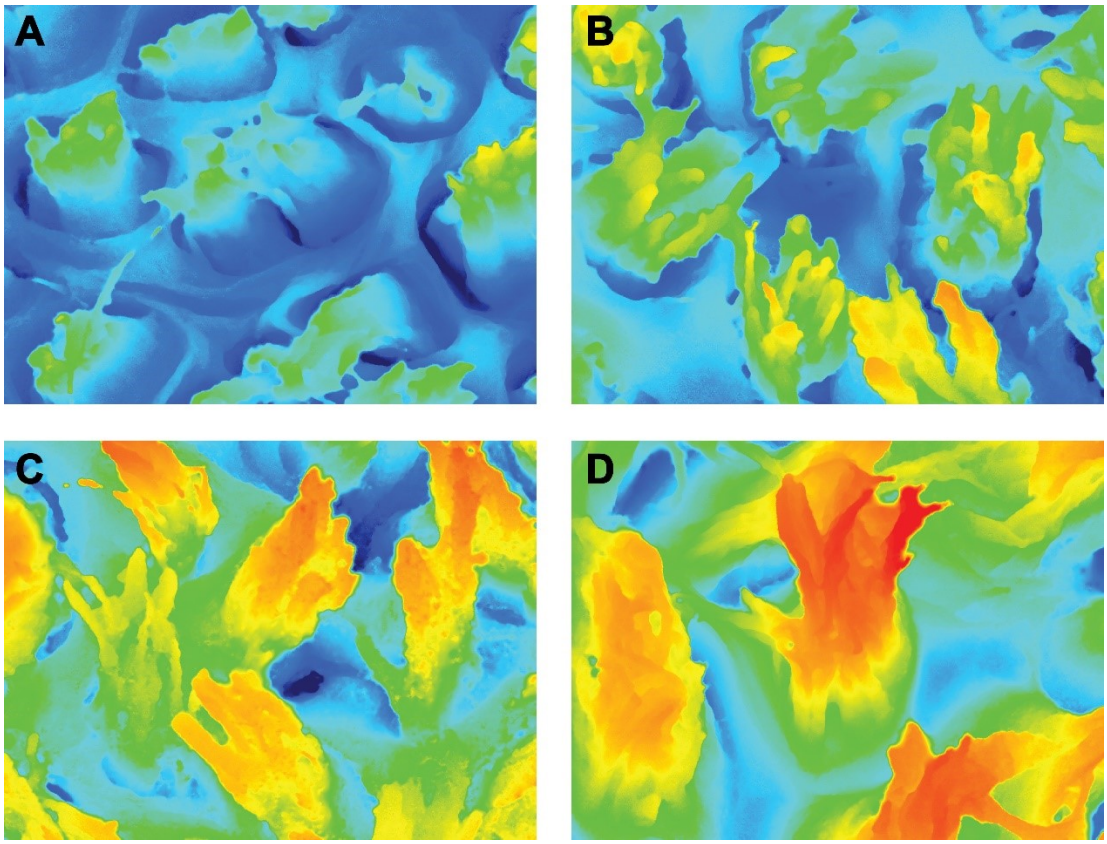

Fig. S2A-D. Visualization of representative papillary length variation across participants. Images include height heat maps from the participants with the shortest papillae (A, $\bar{h}$=462.95μm), the longest papillae (D, $\bar{h}$=1177.21μm), and representative samples participants from the lower and upper quartiles (B, $\bar{h}$=546.24μm and C, $\bar{h}$=818.71μm, respectively). Above images standardized to uniform height scale ranging from dark blue to red for clarity (89.359μm-1086.593μm).

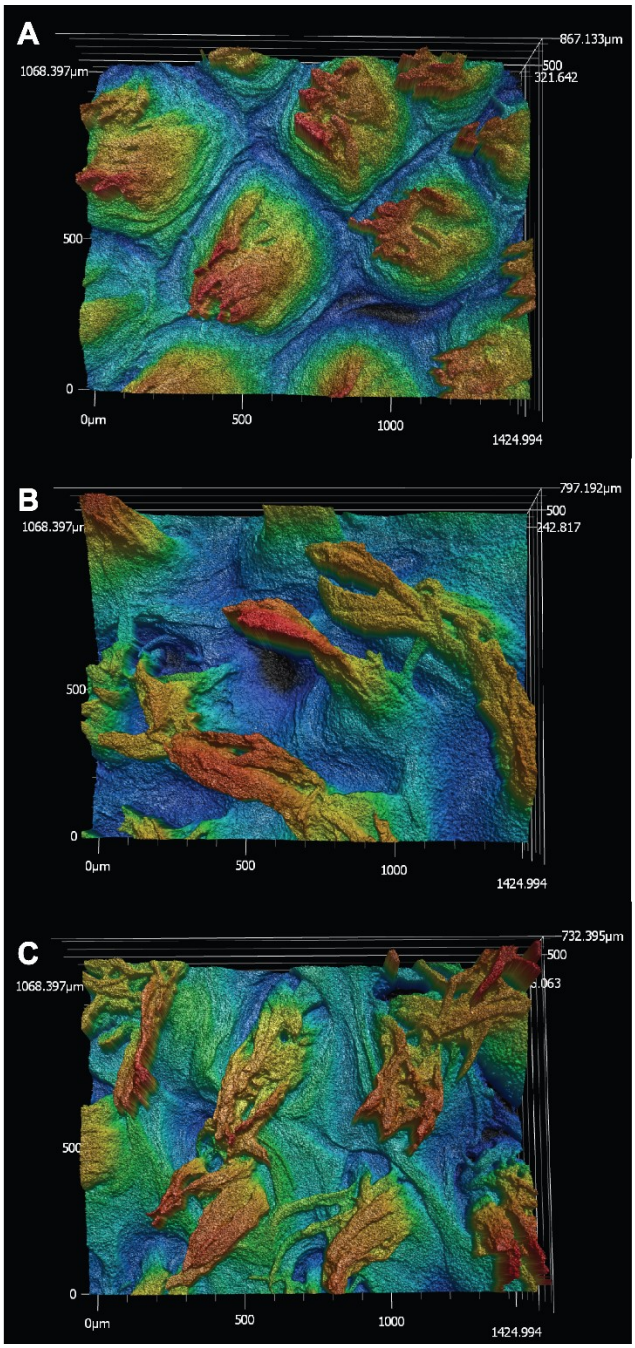

Fig. S3A-C. 3D surface models of tongues of individuals with equivalent PB JNDs. While pictured individuals show a high degree of diversity in structure shape, length, and density all individuals show a similar and high level of acuity (JND =580.88cP, 797.38cP, and 673.75cP, respectively). Multiple different phenotypes appear to be equally successful at discriminating between high-viscosity fluids.

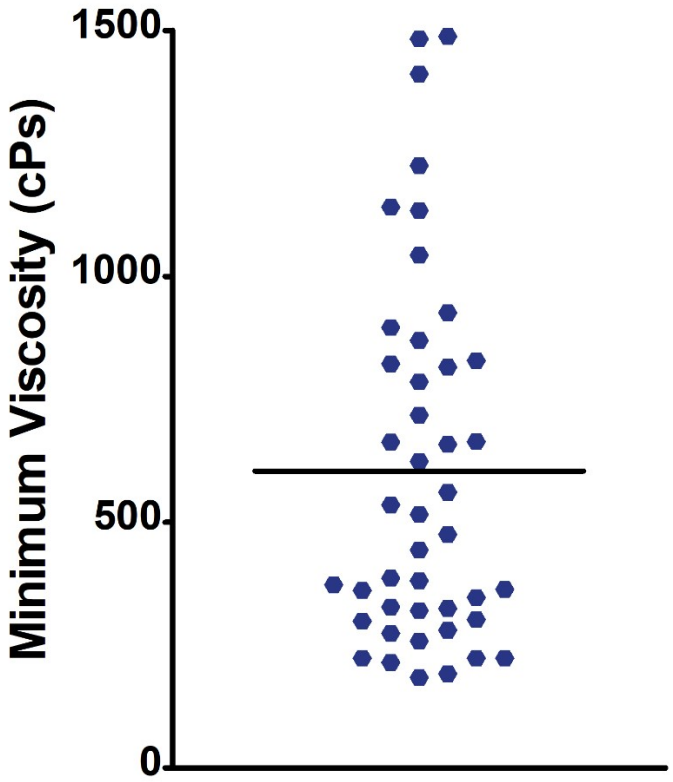

Fig. S4. Modeled minimum viscosity needed to generate 1μm tip displacement. Using each individual's tip displacement at 5860cPs, a theoretical minimum viscosity for the papillary-based perceptual mechanism was determined. Note the wide range of viscosity values that are reflective of the variable papillary geometry. Cutoffs ranged from 183.921-1487.698cPs (Black horizontal line indicates avg. threshold = 604.102 ± 55.777cPs).

SI References

1. S. Tomovich, Z. Peng, C. Yuan, X. Yan, “Quantitative surface characterisation using laser scanning confocal microscopy” in *Laser Scanning, Theory and Applications*, C.-C. Wang, Ed. (2011), pp. 1–30.
2. S. Fu, F. Cheng, T. Tjahjowidodo, Y. Zhou, D. Butler, A non-contact measuring system for in-situ surface characterization based on laser confocal microscopy. *Sensors (Switzerland)* **18** (2018).
3. W. J. Hume, C. S. Potten, The ordered columnar structure of mouse filiform papillae. *J. Cell Sci.* **22**, 149–160 (1976).